

In Situ Band Gap Engineering of Carbon Nanotubes

Vincent H. Crespi* and Marvin L. Cohen

Department of Physics, University of California at Berkeley, Berkeley, California 94720, and Materials Sciences Division, Lawrence Berkeley National Laboratory, Berkeley, California 94720

Angel Rubio

Departamento de Física Teórica, Universidad de Valladolid, E-47011 Valladolid, Spain

(Received 8 May 1997)

Bond rotation defects close the gap in large-gap nanotubes, open the gap in small-gap nanotubes, and increase the density of states in metallic nanotubes. Not only are these defects likely to be present in as-grown nanotubes, but they could be introduced locally into intact nanotubes, thereby opening a new road towards device applications. [S0031-9007(97)03973-2]

PACS numbers: 71.20.Tx, 61.72.Bb, 71.15.Fv, 74.10.+v

The vanishing Fermi surface of a graphite sheet implies either semiconducting and metallic behavior in carbon nanotubes [1] depending on circumferential boundary conditions [2]. Indexing tubes by the number of lattice vectors around a circumference, theory predicts that (n, n) tubes are metals, $(n, n + 3i)$ tubes (with i an integer) are small-gap semiconductors with $E_{\text{gap}} \propto \frac{1}{R^2}$ and other tubes have larger gaps proportional to $\frac{1}{R}$. This classification, based on band folding and hybridization, depends critically on the size and location of the graphitic Fermi points.

Progress towards measurements on nanotubes of a well-defined index motivates a reassessment of these elegant theoretical predictions for pure nanotubes. It has already been shown that a pentagon-heptagon defect creates a metal/metal, metal/semiconductor, or semiconductor/semiconductor heterojunction [3] between two perfect semi-infinite half-tubes with different indices. This defect causes a global change in structure and hence cannot be induced locally. In this Letter we analyze topological defects *within a single nanotube of well-defined index*, defects which allow band gap modification beyond that expected for perfect nanotubes.

A $\frac{\pi}{2}$ local bond rotation [4] in a graphitic network creates two pentagons and two heptagons,



a Gaussian curvature quadrupole which does not change the global tube index. A bond rotation in a typical carbon nanotube costs 4–5 eV with a kinetic barrier of 7 eV against a planar rotation [5], large enough to guarantee metastability at room temperature [6].

To understand the electronic effects of bond rotation in nanotubes we first examine pentaheptite, a planar carbon material composed entirely of pentagons and heptagons [7]. Within the local density approximation (LDA) pentaheptite is 0.33 eV/atom higher in energy than an isolated graphite sheet. The energetic cost of distorting the sp^2

framework in pentaheptite is slightly lower than in C_{60} , bolstering the notion that bond rotations are plausible entities. Unlike a single sheet of graphite, pentaheptite within both LDA and tight binding (TB) is a metal with a substantial Fermi surface around the Γ point and 0.1 states per eV per atom at the Fermi energy [8]. Within an extended zone scheme, increasing the density of bond rotation defects in a graphite sheet should continuously transform the Fermi points of graphite at the edges of the Brillouin zone into the Fermi surface of pentaheptite around Γ . Since the circumferential boundary conditions of a nanotube slice the zone quite thinly, this expansion and motion of the Fermi surface has dramatic effects on tube electronic structure even at low defect concentrations.

To flesh out these intuitive observations we have performed extensive TB and LDA calculations for defective nanotubes of each electronic flavor. The (7,0) tube is a semiconductor with a large band gap of ~ 1 V in TB. The (5,5) tube is a metal with 0.05 states per eV per atom at the Fermi energy. The (9,0) tube is a semiconductor with a small hybridization-induced gap of ~ 0.07 V. TB calculations using the parametrization of Ref. [9] were reinforced by *ab initio* norm-conserving [10] pseudopotential calculations in the LDA [11]. The LDA calculations used a supercell with well-isolated tubes 5.5 Å apart. An energy cutoff of 40 Ry in a plane-wave basis yielded band energies converged to 0.04 eV. An LDA cross-check of the TB results is most important in the smallest tubes, in which curvature-induced hybridization can reduce the gap [12]. The (9,0) and (5,5) tubes are large enough that LDA and TB results for the electronic structure around the Fermi level are very similar.

Coordinates of defective tubes were generated by rotating one, two, or three bonds in a supercell of a perfect tube and relaxing the resulting structure with tight binding molecular dynamics (TBMD) [13], allowing the axial unit cell length to vary. The roles of curvature-induced hybridization and periodic boundary conditions were clarified by unrolling the tube unit cells and performing similar calculations on the resulting flattened sheets of

defective graphite. Unless otherwise noted, a line through the heptagons [pentagons] is parallel to the tube axis in the (7,0) and (9,0) [(5,5)] tubes. When two defects inhabit the supercell they are spaced evenly on opposite sides of the tube. When three defects inhabit the supercell they are distributed uniformly.

The pure (7,0) tube has a large gap which is reflected in the (7,0)-derived planar graphite supercell by the large distance between the Fermi points and the Γ -X line, the line comprising the k values allowed by circumferential boundary conditions in the corresponding tube. Rotating one bond in two hundred reduces the tube gap by 30%–40% (Fig. 1). The mechanism for gap closure in the tube is best understood via the sheet calculations (Fig. 2). Bond rotation defects in the sheet move the Fermi surface closer to the Γ -X line, closing the gap of the corresponding nanotube. Two defects within a 56-atom unit cell suffice to close the tubular gap. Curvature-induced hybridization aids this metallization: The corresponding sheet at this defect density still maintains a small gap. Within an extended zone scheme based about the original graphitic cell with a two-atom basis, the gap closes as the Fermi surface moves from the K point towards the closest line of allowed k values in the direction of the Γ point (see Fig. 3). Since the lines of allowed k values miss the Fermi points by a wide margin in the pure (7,0) tube, any motion and expansion of the Fermi points upon introduction of defects is likely to close the gap. LDA calculations yield a similar 40% reduction in the band gap under 1% bond rotation, but the absolute values of the band gaps are smaller due to σ^* - π^* hybridization not included in the TB parametrization [12].

Are these results sensitive to the locations and alignments of the defects? We recalculated the electronic

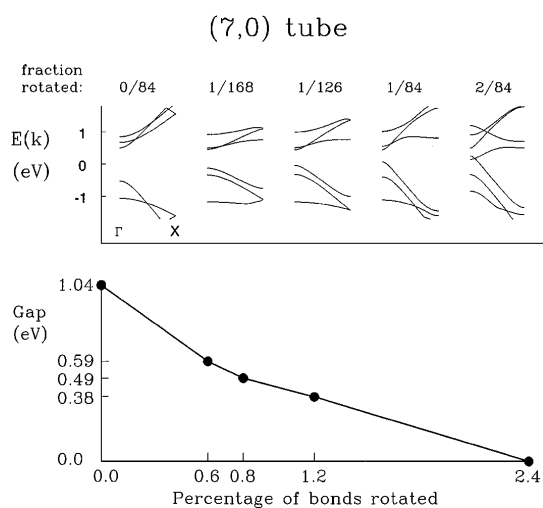


FIG. 1. Evolution of the band structure $E(k)$ and gap of (7,0) tubes upon increasing the concentration of bond rotation defects. Fractions indicate the number of rotated and unrotated carbon-carbon bonds within the supercell.

structures of the 84-atom (126-bond) sheet and tube with the defect at a $\frac{\pi}{3}$ angle to the tube axis. The defects decrease the gap by 15%, compared to 60% for parallel alignment. Similar but smaller differences arise when the defects alternate from one side of the tube to another in a doubled unit cell. Although the size of the gap reduction changes, the qualitative picture is preserved, with bond rotation defects closing the gap. The robustness of the continuous evolution in electronic structure through systems of different sizes with different defect arrangements in both tight binding and the LDA suggests that this mechanism of defect-induced metallization has general relevance for large-gap carbon nanotubes.

Since one line of allowed k values in an (n, n) tube passes from the extended zone graphitic Γ point to the K point, the motion of the Fermi point along this line from K to Γ upon introduction of bond rotation defects should not open a gap. We explore this situation through calculations on defective (5,5) nanotubes. As expected, defects do not open a gap, but instead increase the density of states at the Fermi level as the large π - π^* band dispersion decreases (Fig. 4). The corresponding sheet calculations show the Fermi points moving along the Γ -X line with band dispersion very similar to that of the associated tubes. When the defects in neighboring cells are almost touching, a flat impurity band crosses the Fermi level. Although the electron-phonon matrix elements in

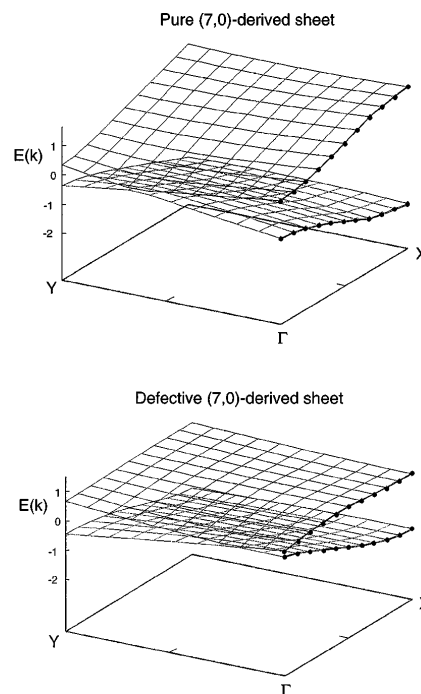


FIG. 2. Two bond rotation defects in a 56-atom graphitic supercell move the Fermi surface towards the Γ point along the Γ -Y line of the sheet Brillouin zone. Since the periodic boundary conditions in the corresponding tube pick out the Γ -X line, this motion of the sheet Fermi surface closes the gap of the defective tube.

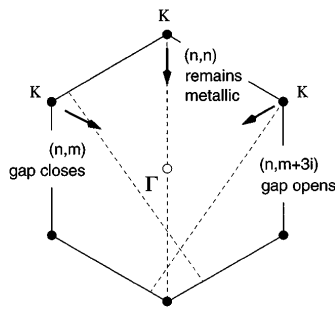


FIG. 3. Schematic diagram showing the evolution of the electronic structure of a graphitic sheet upon introduction of bond rotation defects. The dashed lines show allowed k values for large-gap, small-gap, and metallic tubes.

small tubes should be moderately large [14], a defect-free (n, n) tube is a very poor BCS superconductor unless the density of states is increased by doping the system away from the π - π^* crossing. Using bond rotation defects to increase the density of states may have an advantage over chemical doping since alkali doped superconducting C_{60} and graphite are not air stable.

Motivated by experiment, we also examine bond rotation defects in $(10,10)$ tubes, the most common component of recently synthesized single-walled nanotube bundles [15]. One bond rotation defect aligned with the axis of a 160-atom supercell breaks the electron-hole symmetry while shifting and splitting the Van Hove singularities in the density of states on a scale of 0.5 eV. New states associated with the atoms in the pentagons and heptagons appear within the metallic plateau near the Fermi energy and increase the density of states by roughly 25%.

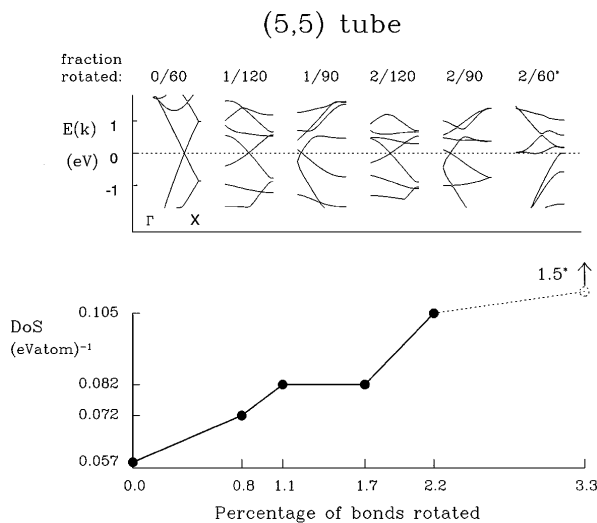


FIG. 4. Evolution of the band structure $E(k)$ and density of states of $(5,5)$ tubes upon increasing the concentration of bond rotation defects. (*) Two rotated bonds within a 60-atom unit cell yield a flat defect band with an anomalously high density of states of 1.5 per atom per eV.

Motion and expansion of the graphitic Fermi points can also open the gap of the corresponding tube. The $(n, n + 3i)$ nanotubes have small hybridization-induced gaps; the graphitic Fermi point is essentially adjacent to the line of allowed k values. In these tubes the defect-induced evolution of the extended two-dimensional zone Fermi surface from K to Γ can pull the Fermi surface away from the adjacent line of allowed k values, thereby opening a gap. This process is visible in the electronic structure of the defective $(9,0)$ tube, in which the gap opens from 0.07 to 0.5 eV as the defect concentration increases from zero to two bonds in 108 (Fig. 5). Thereafter, the extended-zone two-dimensional Fermi surface approaches the next line of allowed k values and the gap closes. The bond rotation also breaks the degeneracy of the π and especially the π^* bands. Similar gap openings are expected in other defective $(n, n + 3i)$ tubes.

Are these defects visible in real space? Bond rotation defects with the line through the centers of the heptagons parallel to the tube axis form only a slight (0.2 Å) outward pucker in the side of a nanotube. However, when a line between the pentagons is parallel to the tube axis, the positive curvature of the pentagons forms a divot which is compatible with optimally oriented saddles of negative curvature from the heptagons, yielding a divot approximately 0.9 Å deep. Although the distortion is large, the number of atoms involved is small, suggesting that the defects are difficult to see in a transmission electron microscope. Alternatively, a scanning probe microscope could resolve these defects on the surface of a nanotube. Recent scanning tunneling microscopy experiments have spectroscopically resolved purely pentagonal defects near the tips of carbon nanotubes [16].

The density of bond rotation defects would be small in thermodynamic equilibrium. At 4–5 eV per defect

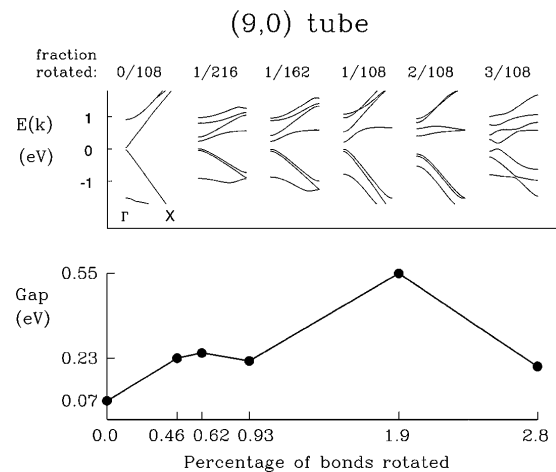


FIG. 5. Evolution of the band structure $E(k)$ and gap of $(9,0)$ tubes upon increasing the concentration of bond rotation defects. The gap is maximal when two defects occupy a 108-bond supercell.

thermal equilibrium at 3000–4000 K yields 1 in 10^5 bonds rotated. At these low concentrations bond rotations would affect the electronic structure within a series of ~ 200 atom patches around each defect. But tube growth is nonequilibrium. Energetically comparable but much more visible defects, i.e., isolated pentagons and heptagons, are often seen in transmission electronic microscopy of multiwalled tubes. In addition, and perhaps more importantly, bond rotation defects could be added *in situ* to as-grown nanotubes.

Theoretical and experimental studies of knock-on beam damage in a transmission electron microscope show that carbon atoms are most easily ejected from a nanotube by a 15 eV kinetic energy transfer perpendicular to the local sp^2 plane [17]. TBMD calculations also show an upper limit of 7 eV on the barrier to bond rotation [5]. By tuning a particle beam so that the maximum knock-on kinetic energy transfer is below 15 but above 7 eV, one should be able to selectively create bond rotation defects without threatening the structural integrity of the tube. These defects would form preferentially on the sides of the tube perpendicular to the beam direction, yielding two lines of defects reminiscent of the defect arrangements considered in our calculations.

A carbon nanotube metallized by defects might show stronger one-dimensional effects than a defect-free metallic (n, n) nanotube. Anderson localization is clearly favored by a disordered defect potential and also by the filamentary nature of the electronic states near the Fermi level in a nanotube at the edge of defect-induced metallization. The more spatially confined nature of the electronic states near the Fermi energy may also enhance the interelectron Coulomb matrix elements.

In conclusion, the delicate interplay of pointlike Fermi surfaces and periodic boundary conditions opens the carbon nanotubes to dramatic variations in electronic structure upon perturbation of the sp^2 framework. In a graphitic sheet the density of bond rotation defects controls the size and location of the Fermi surface. In a tube the density of defects determines the size of the band gap or the density of states at the Fermi level. Not only are low concentrations of these defects expected in as-grown tubes, but higher concentrations could be realized by controlled irradiation, thereby tuning the electronic, transport, and field emissive properties of sp^2 based nanotubes.

V.H.C. and M.L.C. acknowledge National Science Foundation Grant No. DMR-9520554 and Office of Energy Research, Office of Basic Energy Sciences, Materials Sciences Division of the U.S. Dept. of Energy Contract No. DE-AC03-76SF00098. A.R. acknowledges DGES Grant No. PB95-0720-C02-01 and DGICYT Grant No. PB95-0202, European Community TMR Contract No. ERBFMRX-CT96-0067 (DG12-MIHT), and Junta de Castilla y León Grant No. VA25/95.

*Present address: 104 Davey Lab, Department of Physics, The Pennsylvania State University, University Park, PA 16802.

Electronic address: <http://oak.phys.psu.edu>

- [1] S. Iijima, *Nature (London)* **354**, 56 (1991).
- [2] N. Hamada, S. Sawada, and A. Oshiyama, *Phys. Rev. Lett.* **68**, 1579 (1992); J.W. Mintmire, B.I. Dunlap, and C.T. White, *Phys. Rev. Lett.* **68**, 631 (1992); R. Saito, M. Fujita, G. Dresselhaus, and M.S. Dresselhaus, *Appl. Phys. Lett.* **60**, 2204 (1992).
- [3] L. Chico, V.H. Crespi, L.X. Benedict, S.G. Louie, and M.L. Cohen, *Phys. Rev. Lett.* **76**, 971 (1996); R. Saito, G. Dresselhaus, and M.S. Dresselhaus, *Phys. Rev. B* **53**, 2044 (1996); J.C. Charlier, Ph. Lambin, and T.W. Ebbesen, *Phys. Rev. B* **53**, 11 108 (1996).
- [4] A.J. Stone and D.J. Wales, *Chem. Phys. Lett.* **128**, 501 (1986).
- [5] The actual barrier might be lower due to out-of-plane motion. The barrier in a nanotube is probably between the 5.4 eV barrier for the related Stone-Wales transformation [5] in C_{60} [J.-Y. Yi and J. Bernholc, *J. Chem. Phys.* **96**, 8634 (1992)] and the 10.4 eV barrier for bond rotation in flat graphite [T. Kaxiras and K.C. Pandey, *Phys. Rev. Lett.* **61**, 2693 (1988)].
- [6] Molecular dynamics simulations show that these defects can anneal out in a few picoseconds at the growth temperature of 3000–4000 K; P.A. Marcos, M.J. López, A. Rubio, and J.A. Alonso (to be published).
- [7] V.H. Crespi, L.X. Benedict, M.L. Cohen, and S.G. Louie, *Phys. Rev. B* **53**, 13 303 (1996).
- [8] Since a line of allowed k values always passes through Γ , pentaheptitic tubes are always band metals. Note that metallization due to bond rotation is distinct from the metallization of very small tubes due to curvature-induced $\sigma^*-\pi^*$ hybridization [12].
- [9] D. Tomanek and S.G. Louie, *Phys. Rev. B* **37**, 8327 (1988). We use their sp^3 Slater-Koster parameters with a linear interpolation between graphitic first and second-neighbor parameters.
- [10] N. Troullier and J.L. Martins, *Phys. Rev. B* **43**, 1993 (1991).
- [11] J.P. Perdew and A. Zunger, *Phys. Rev. B* **23**, 5048 (1981).
- [12] X. Blase, L.X. Benedict, E.L. Shirley, and S.G. Louie, *Phys. Rev. Lett.* **72**, 1878 (1994).
- [13] C.H. Xu, C.Z. Wang, C.T. Chan, and K.M. Ho, *J. Phys. Condens. Matter* **4**, 6047 (1992).
- [14] L.X. Benedict, V.H. Crespi, S.G. Louie, and M.L. Cohen, *Phys. Rev. B* **52**, 14 935 (1995).
- [15] A. Thess, R. Lee, P. Nikolaev, H. Dai, P. Petit, J. Robert, C. Xu, Y.H. Lee, S.G. Kim, A.G. Rinzler, D.T. Colbert, G.E. Scuseria, D. Tománek, J.E. Fischer, and R.E. Smalley, *Science* **273**, 483 (1996).
- [16] D.L. Carroll, P. Redlich, P.M. Ajayan, J.C. Charlier, X. Blase, A. De Vita, and R. Car, *Phys. Rev. Lett.* **78**, 2811 (1997).
- [17] V.H. Crespi, N.G. Chopra, M.L. Cohen, A. Zettl, and S.G. Louie, *Phys. Rev. B* **54**, 5932 (1996).